Khattak, YH.; Baig, F.; Toura, H.; Harabi, I.; Beg, S.; Marí, B. (2019). Single step electrochemical deposition for the fabrication of CZTS kesterite thin films for solar cells. Applied Surface Science. 497:1-7. https://doi.org/10.1016/j.apsusc.2019.143794

Y. H. Khattak et al, Applied Surface Science 497 (2019) 143794
DOI: 10.1016/j.apsusc.2019.143794

Single Step Electrochemical Deposition for the Fabrication of CZTS Kesterite Thin Films for Solar Cells

Yousaf Hameed Khattak[1,2] , Faisal Baig[1,2], Hanae Toura[1,3], Imen Harabi[1], Saira Beg[4], Bernabé Marí Soucase[1]

[1] School of Design Engineering, Universitat Politécnica de Valencia, Camí de Vera, Spain

[2] Electrical Engineering Department, Federal Urdu University of Arts, Science and Technology Islamabad, Pakistan

[3] Laboratory Materials and Environment Engineering: Modeling and Application, Department of Chemistry, University Ibn Tofail, Kenitra, Morocco

[4] COMSATS University Islamabad, Pakistan

Corresponding Author: * yousaf.hameedk@gmail.com

Abstract

The high absorption coefficient and direct optical band gap of a kesterite Cu_2ZnSnS_4 (CZTS) makes it very promising absorber material in the manufacturing of high efficiency and low-cost thin film photovoltaic cells. Single step electrochemical deposition of CZTS quaternary compound thin films on Indium tin oxide (ITO) substrates is reported in this work. The films were obtained from aqueous solutions at room temperature. The key objective of this work is to examine the effect of annealing temperature on CZTS thin films. Sulfurization of thin films were performed under different temperature range from 400℃ to 550℃. Good crystal structure was achieved at temperature 500℃ with the complexing agent of trisodium citrate. Deposited films material composition was evaluated by analyzing UV-visible spectroscopy, EDS, FE-SEM and XRD. The thin film with good morphological, structural and optical (1.51eV) properties was achieved at temperature 500℃. The results reported in this work will provide an imperative guideline for efficient low-cost design of CZTS thin films.

Keywords: Cu_2ZnSnS_4, $CZTS$, Kesterite, Solar cell, Electrochemical deposition, Photovoltaics

1. Introduction:

The photovoltaic cell made from semiconductor materials plays a momentous role in power production. The solid-state semiconductor photovoltaic devices have emerged as a newer and a relatively sustainable energy source. For production purposes, thin film technology is used as the efficient and cost-effective solar cell technology. This technology is an excellent and exceptional topic of intense research and also suitable for large and low scale device application [1]. Thin film photovoltaic technologies are based on various types of light absorbers semiconductor materials. Historically in the thin film technology, amorphous silicon-based solar cells played a momentous role. Researchers move towards cadmium telluride $CdTe$ and copper indium gallium selenide $CIGS$ based thin-film solar cell materials [2]. Commercially these materials are used for the production of thin film solar cells because of high absorption coefficient $> 10^4 cm^{-1}$, excellent optical and electrical properties and high power conversion efficiency [3,4]. For many decades great effort has been done on the optimization of $CIGS$ and $CdTe$-based devices. The scalability of technology is limited for commercial use because of the rising cost and toxic nature of content cadmium (Cd) in $CdTe$ absorber and the scarcity of tellurium (Te), gallium (Ga) and indium (In). The toxic nature restricts the further advancement of these photovoltaic cells and the rare materials, gallium (Ga) and indium (In) used in these photovoltaic cells also increase the manufacturing cost. Therefore, the commercial production of $CIGS$ based photovoltaic cell is limited [5,6].

Currently intensive research is conducting on Cu_2ZnSnS_4 $(CZTS)$, $Cu_2ZnSnSe_4$ $(CZTSe)$ and sulfur-selenium alloy $Cu_2ZnSn(S_xSe_{1-x})_4$ $(CZTSSe)$ for the development and production of low cost sustainable thin film solar cells. These materials drawing consideration because of exceptional electrical and optical properties for photovoltaic applications. These absorber materials are copper based nontoxic semiconductor materials. They are a good substitute for chalcopyrite absorbers when replaced gallium (Ga) with tin (Sn) and indium (In) with comparatively inexpensive zinc (Zn) in the $CIGS$ absorbers [7–10]. The optimum direct band gaps, outstanding features and efficient performance of these kesterite materials made them very fascinating in the thin film's community. Several techniques have been used to synthesize the $CZTS$ kesterite thin films like spin coating [11], sol–gel [12], electrochemical deposition [13], spray pyrolysis [14], doctor-blade coating [15], co-sputtering [16,17], chemical bath deposition [18], SILAR [19], photochemical deposition [20]. The highest power conversion efficiency (PCE) achieved for Se rich $CZTSSe$ based solar cell was 12.6% prepared by hydrazine-based solution deposition process [21]. Because hydrazie is highly toxic and

intensive care should be taken while handling hydrazine using proper protective equipment and this add to the cost of solar cell fabrication. 11.6% efficient $CZTSSe$ thin film solar cell was fabricated using thermal co-evoporation method [22] and via electrodepostion a PCE of 7% was achieved for $CZTSe$ based solar cell [23]. For pure sulfide based kesterite solar cell with PCE of 11.01% and having high open circuit voltage of 730.6 meV was achieved using co-sputtring method with heat treatment of fabricated samples [24]. Whereas $CZTS$ with PCE of 8.4% was also achieved by preheating an electrodepsited electrode at 310°C in an evacuated borosilicate glass ampoule before sulfrization [25]. Among all these techniques we find electro chemical deposition interesting for kesterite application because many composite metal alloys can be deposited on a large surface area with controlled thickness [26,27]. Although in single step electrodeposition of $CZTS$ is quite difficult to control because the metal alloys $Cu - Zn - Sn - S$ presents different oxidization reduction potential [28,29]. To control the oxidization and reduction potential for metal alloys complexing agent play a vital role in bath solution [30,31] because the key factors for kesterite performance are deposition potential, crystalline structure and stoichiometry [32,33]. There is an empirical rule, that Cu poor and Zn rich based $CZTS$ thin film reported high conversion efficiency. The ratio for metal alloys should be ranged between 0.70 to 1.20 ($Cu/Zn + Sn$) [34–36].

The effect of complexing agent concentration on annealing temperature with optical, structural and morphological characterization were investigated in this research work. In order to obtain cost effective $\boldsymbol{CZTS}$ thin films by single bath electrodeposition technique, we examined the effect of the addition of the complexing agent $\boldsymbol{C_6H_5Na_3O_7}$ on the annealing temperature, which creates the originality of this study.

2. Experimental section

CZTS kesterite precursor film were electrochemically deposited on indium tin oxide (ITO) coated glass substrate having $\boldsymbol{1 \times 2.5\ cm^2}$ area of deposition. 50 milli litter aqueous solution containing 0.02M copper sulfate pentahydrate $\boldsymbol{CuSO_4.5H_2O}$, 0.01M zinc sulfate monohydrate $\boldsymbol{ZnSO_4.H_2O}$, 0.01M tin sulfate $\boldsymbol{SnSO_4}$, and 0.02M sodium thiosulfate $\boldsymbol{Na_2S_2O_3}$ were used as electrolyte. To keep the pH of electrolyte around 5, 0.1M tartaric acid ($\boldsymbol{C_6H_6O_6}$) was added in CZTS precursor. 0.2M trisodium citrate ($\boldsymbol{C_6H_5Na_3O_7}$) was used as complexing agent. Electrochemical deposition was carried out by using three-electrode setup in Autolab PGSTAT302N potentiostatic. Where ($\boldsymbol{Ag/AgCl}$) saturated calomel electrode as the reference electrode, platinum wire ($\boldsymbol{Pt}$) as a counter electrode, $\boldsymbol{ITO}$ were used as a working electrode. The working electrode is immersed in the precursor solution. Schematic diagram of

electrochemical deposition setup is shown in Figure 1. CZTS precursor layer were deposited by using chronoamperometry technique at -1.05V potential (vs. Ag/AgCl). Without stirring deposition was taken for 30 min at room temperature. After deposition process ended, CZTS deposited films were rinsed with deionized water and after that at room temperature they were dried in air. To get the required peaks from the deposited films, films were annealed at different temperatures by applying sulfurization. For the sulfurization process we use tubular setup, in which graphite posts are used for the holding of deposited films and sulfur powder ($\boldsymbol{S}$) was also used. Annealing process was done with the presence of argon ($\boldsymbol{Ar}$) gas in tubular setup within the temperature variant from 400°C to 550°C for 40 min.

CZTS films samples structural characterization was carried out by using Rigaku Ultima IV Ray Diffractometer (XRD), $\boldsymbol{CuK\alpha}$ radiation ($\boldsymbol{\lambda = 1.54060}$ Å) in the Bragg-Bentano configuration. Field emission scanning electron microscopy (FE-SEM) analysis was done to examine the morphology and energy dispersive X-ray (EDS) analysis was done to investigate the chemical composition of the CZTS deposited samples with $\boldsymbol{0.2\ M}$ concentration of complexing agent. These analyses were performed by using Zeiss ULTRA 55 model equipped with an In-Lens SE detector. Raman spectroscopy of different annealed samples were recorded by using Horiba Jobin Yvon LabRAM HR spectrometer equipped with thermoelectrically cooled Electronically enhanced Multichannel Charge Coupled Device (EMCCD) and an edge filter that cuts Raman signals below ~35 $\boldsymbol{cm^{-1}}$. Solid-state green laser emitting at $\boldsymbol{533\ nm}$ with a resolution of roughly $\boldsymbol{1\ cm^{-1}}$ was used. The optical properties of CZTS films were evaluated by using Ocean Optics HR4000 UV-Visible spectrophotometer coupled with an integrating sphere (to collect both specular and diffuse transmittance). Optical band gap ($\boldsymbol{Eg}$) estimated from Tauc Equation is $\boldsymbol{\alpha h\nu = A\,(h\nu - Eg)^n}$ where n is ½ for direct band gap transition and $\boldsymbol{\alpha = 1/t\ ln\,(1/T)}$ relation [37].

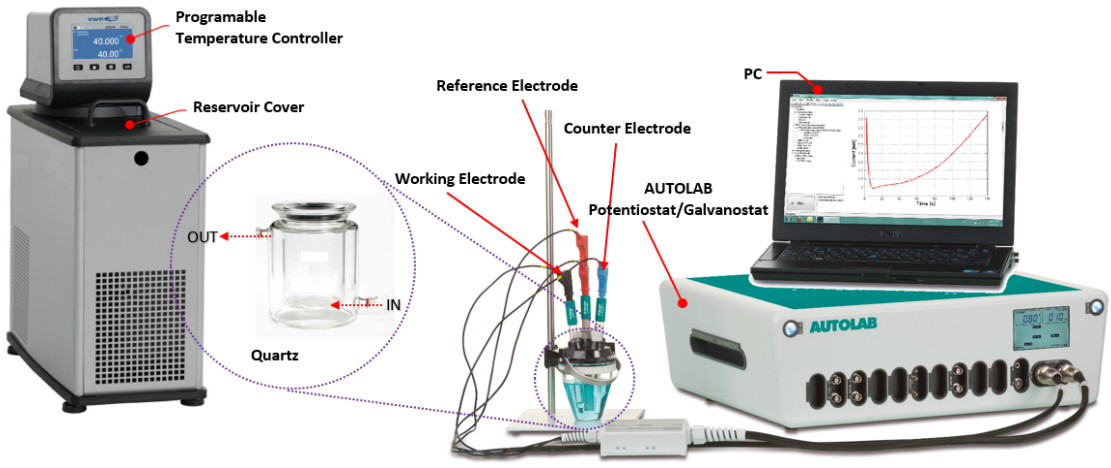

Figure 1 : Autolab PGSTAT 302N potentiostatic setup

3. Result and Discussion

3.1. XRD Analysis

Crystal structure of CZTS precursors samples were examined by using XRD analysis. Figure 2 demonstrates the XRD diffraction spectrum pattern of CZTS as deposited and samples annealed at temperatures of 400°C, 450°C, 500°C and 550°C. The patterns were recorded in 2θ angle range 20°-60°. It can be clearly observed that the as-deposited films exhibit the peaks corresponding to the secondary phase of $\boldsymbol{ZnS}$, $\boldsymbol{Cu_6Sn_5}$ and $\boldsymbol{S}$ [38]. The XRD pattern for annealed sample deposited with 0.2 M concentration of complexing agent shows strong peaks located at 28.31°, 47.10°, and 55.93° corresponding to the (112), (204), and (312) planes with reference JCPDS card #26-0575 [39]. Several weaker peaks were also observed in the annealed samples at point 22.76°, 29.51°, 32.83° for kesterite structure [40–42]. Existence of all peaks for annealed samples are shown in diffraction spectrum.

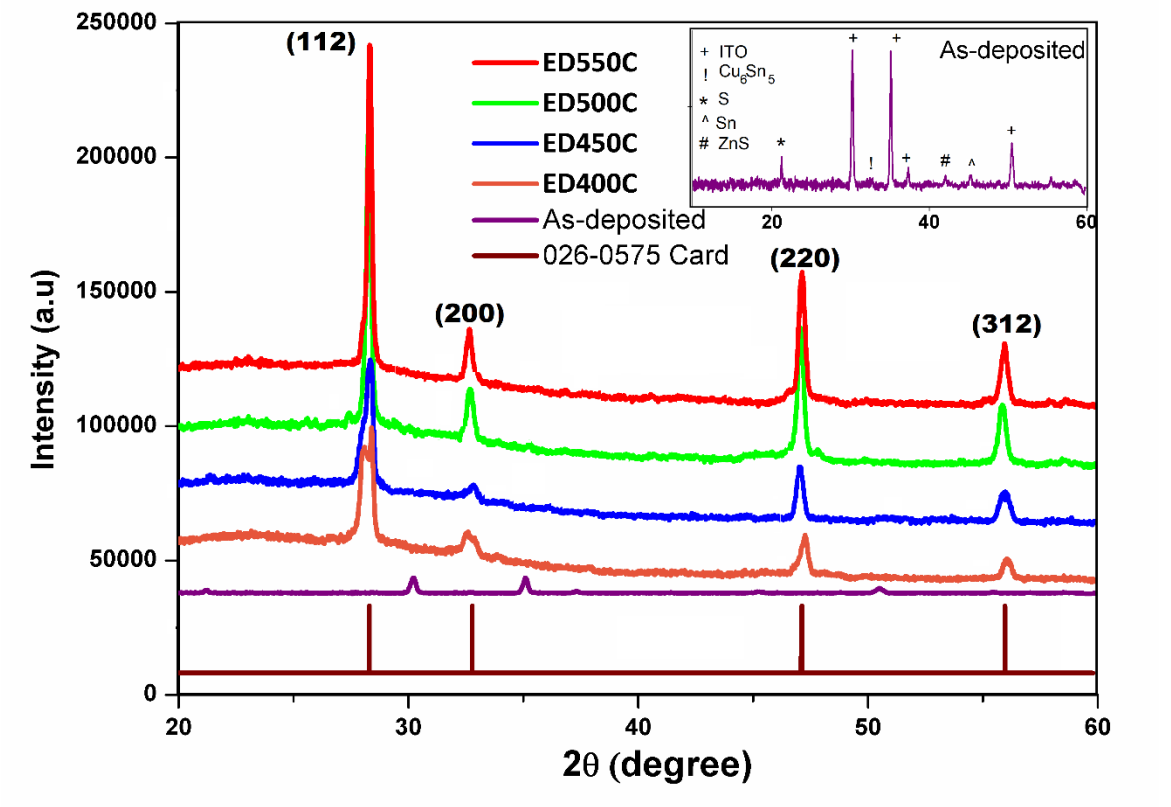

Figure 2: X-ray diffraction spectrum of annealed samples

In the sample ED500C, CZTS kesterite structure thin films reticular planes (112), (220) and (312) are distinctly observed. Moreover, the affinity and intensity of peaks in XRD shows that

the deposition had more crystalline particles. Average value of CZTS thin film crystallite size can be obtained from Debye – Scherrer's equation given in Equation 1[43,44].

$$\boldsymbol{D = (K\lambda/\beta\, Cos\theta)} \quad (1)$$

Where $\boldsymbol{\theta}$ represents the diffraction angle, $\boldsymbol{\beta}$ is the width at half height intensity or full width half maximum (FWHM) of the peak, $\boldsymbol{\lambda}$ is the wavelength of the incident beam, $\boldsymbol{K}$ is Scherrer's constant and usually takes the value 0.9 and $\boldsymbol{D}$ is the crystalline size. XRD analysis states the peaks position, crystallite size and full width at half maximum (FWHM) as given in Table. 1. As cubic ZnS and tetragonal $\mathbf{Cu_2SnS_3}$ has same secondary phases as kesterite CZTS and its hard to distinguish in XRD. Therefore, Raman spectroscopy of different annealed sample was recorded out in range of 200-600 $\mathbf{cm^{-1}}$ and plotted in Figure 3. The main peak of Raman spectra was at 330 $\mathbf{cm^{-1}}$ and this does not correspond to the principal peaks of ZnS and $\mathbf{Cu_2SnS_3}$[45–47].

Table 1 : Structural parameters of the different annealed samples

Sample	Annealing Temperature (°C)	Position of the peak (112)	FWHM β (deg)	Crystallite Size *D* (nm)
ED400C	400	28.2812	0.2289	37.37
ED450C	450	28.3912	0.1891	45.25
ED500C	500	28.3062	0.1848	46.30
ED550C	550	28.2845	0.2057	41.60

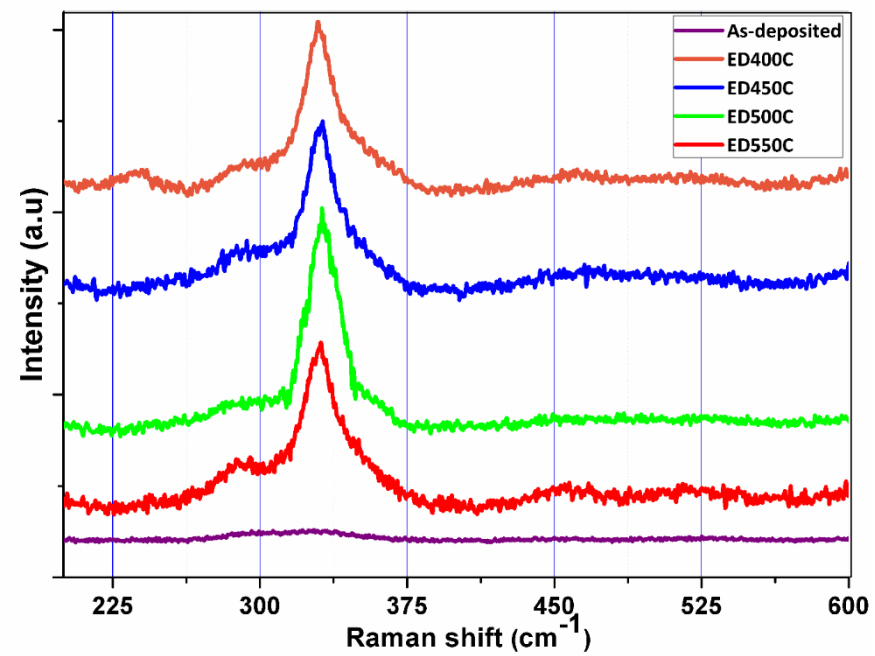

Figure 3: Raman spectra of different CZTS thin films

3.2. FE-SEM and EDS analysis

FE-SEM images of CZTS film as-deposited and samples annealed on different temperature are shown in Figure 4 and Figure 5. Surface morphology of annealed samples strongly dependent on the value of temperature. From Figure 5, we examined that large surface morphological difference is present in the different annealed samples. The morphological studies show that with rising annealed temperature the grain morphology is well define and this effect can be visible by observing Figure 5. The morphology of films ED400C and ED450C shows that the film has a non-uniform surface with the presence of some voids or cavities. Samples ED450C and ED550C have a dense structure with circular grains. FE-SEM morphological analysis of CZTS thin films shows, film surface strongly depends on the annealing temperature and this is confirmed also with the results of XRD given in Figure 2.

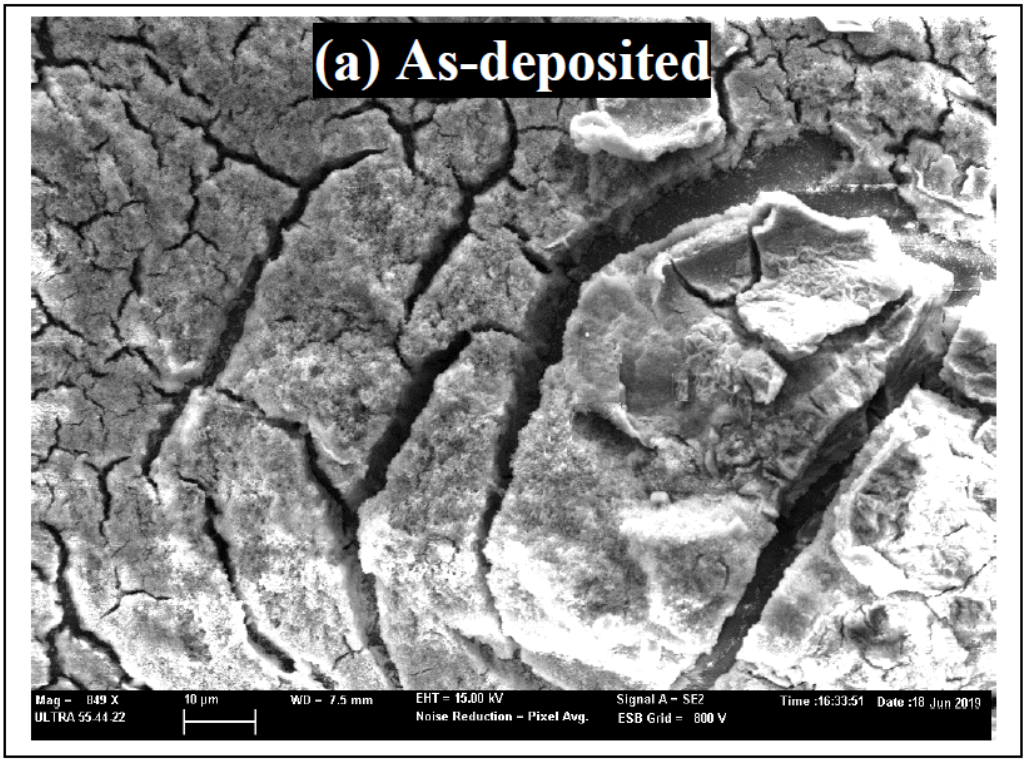

Figure 4: FE-SEM descriptions of as-deposited CZTS film.

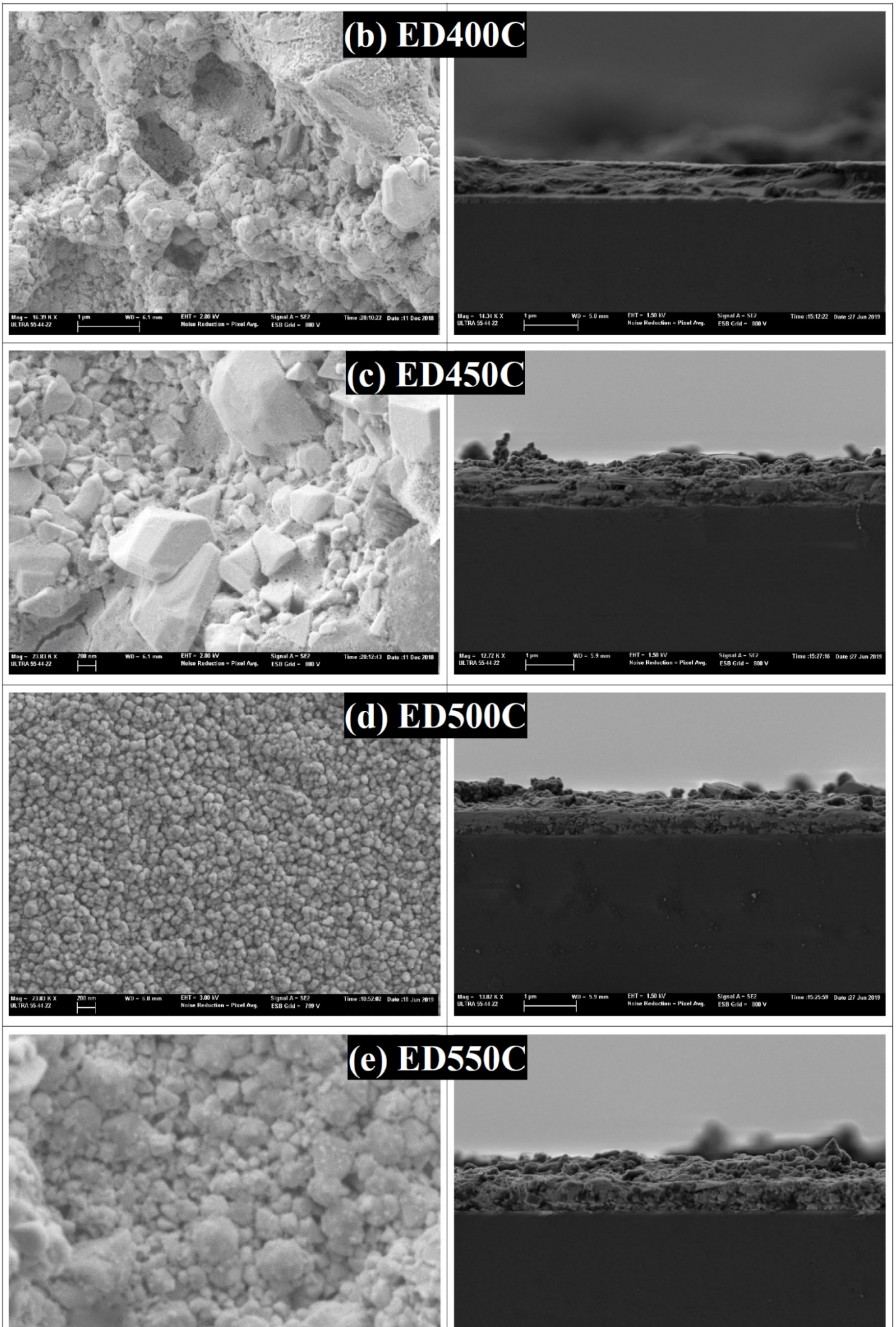
(b) ED400C
(c) ED450C
(d) ED500C
(e) ED550C

Figure 5: FE-SEM descriptions of annealed CZTS film samples with cross-sectional morphology

Identification of elemental composition is done by characterizing the X-rays and the technique used for that is known as X-ray energy dispersive spectroscopy (EDS). Chemical composition can examine in a microscopic area with the help of EDS micro-analyzer. Table 2 explains the EDS analysis data with elemental composition in the electrochemically deposited CZTS thin films with different annealing temperature. From Table 2 with increase in annealing temperature of CZTS thin film, it become more stoichiometric. EDS spectra of different CZTS kesterite thin film samples are shown in Figure 6.

Table 2: CZTS kesterite films composition by EDS analysis

Sample ID	Elements					
	Cu	Zn	Sn	S	Cu/(Zn+Sn)	2Cu + 4(Zn+Sn)/3S
ED400C	34.13	26.22	15.81	23.85	0.81	70.61
ED450C	29.75	14.81	10.98	44.46	1.15	60.27
ED500C	22.82	10.67	16.25	50.26	0.81	46.34
ED550C	25.22	11.33	13.33	50.11	1.02	51.09

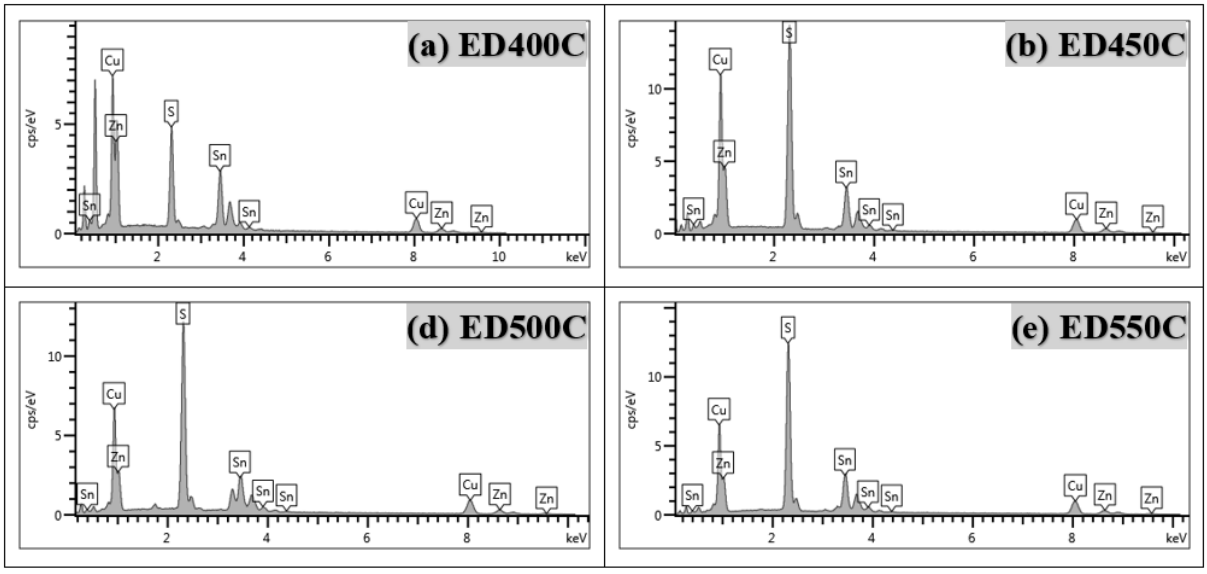

Figure 6: EDS spectrum of annealed CZTS kesterite thin films

Values given for FWHM and crystallite size has a direct effect on strain and dislocation density of film, and this is expressed by the relation given in Equation 2 and 3.

$$\boldsymbol{\delta = (1/D^2)} \quad (2)$$

$$\boldsymbol{\varepsilon = (\beta\, Cot\theta/4)} \quad (3)$$

Results for dislocation density and strain of different annealed CZTS samples are given in Figure 5. From Table 3, with increase in temperature there is a decrease in crystal strain up to

a value of 500℃ but at 550℃ there is an increase in strain indicating imperfection in crystal lattice. The results presented for strain indicates columnar grain growth of crystals as shown in Figure 5.

Table 3: Dislocation density and strain

Temperature (℃)	**δ (Dislocation density) 10^{14} lin.m^{-2}**	**ε (strain)**
400	7.16	0.106367
450	4.88	0.08747
500	4.67	0.08578
550	5.78	0.095569

3.1. UV-visible spectroscopy

Measurement of the band gap energy of the electrochemically deposited CZTS kesterite thin films annealed on different temperature was done on UV visible spectroscopy by using Ocean Optics HR4000 UV-Visible spectrophotometer coupled with an integrating sphere (to gather specular and diffuse transmittance). At room temperature optical absorption spectra recorded in the wavelength for the CZTS kesterite thin films taken was ranging from 450 nm to 1000nm. Transmission spectrum of deposited CZTS films are shown in Figure 7. Optical band gap energies can be determined from the transmittance data.

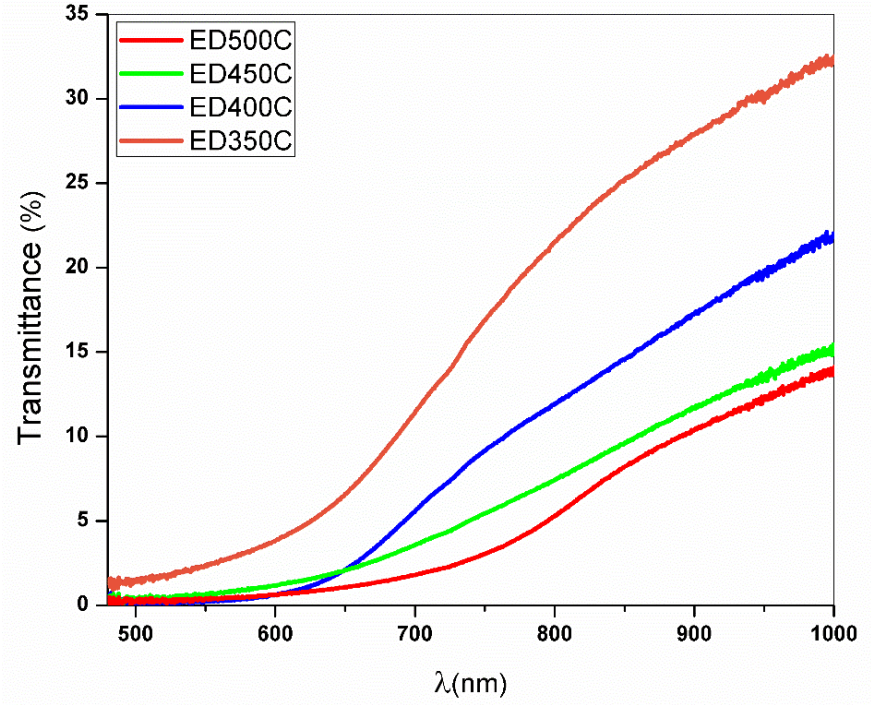

Figure 7: Transmittance spectrum of annealed CZTS kesterite thin films

Variation of $(\boldsymbol{ahv})^2$ as a function of photon energy ($\boldsymbol{hv}$) for deposited CZTS films at a different temperature of annealing. Photo conversion efficiency of solar cell is highly depended upon the material band gap energy. Determining the fundamental band gap energies are possible due to the difference between conduction and valence band levels. The band gap energies are determining with the help of optical absorption spectra. It can be measured by the Tauc's relation between energy and absorption and given in Equation 4

$$(\boldsymbol{\alpha hv})^2 = \boldsymbol{A(hv - Eg)} \qquad (\mathbf{4})$$

where ν is the incident photon frequency, h is the Planck's constant, α is the absorption coefficient, n is equal to 1/2 for a direct transition, and to 2 for an indirect transition E_g is the optical band gap, A is a constant. Electrochemically deposited CZTS kesterite thin films band gap energy is shown in Figure 8. The graph was taken between hv and $(\alpha hv)^2$ and the band gap energy was plotted by drawing a tangential line that extrapolate the linear part of the energy spectrum [48]. Figure 8. shows that different annealed CZTS thin films band gap energies are ranged between $1.48eV$ and $1.61eV$ and rising in annealing temperature decreases the band gap. The grain size, crystallinity and modification of the material structural properties played a momentous role in the variation of optical properties [49]. The band gap energy of samples ED400C, ED450C, ED500C and ED550C are $1.61\ eV$, $1.54\ eV$, $1.51\ eV$ and $1.48\ eV$ respectively. Figure 8 confers that the electrochemically deposited sample ED500C have an optimal band gap value which is near to the optimum band gap for designing the high-power conversion efficiency from solar cell.

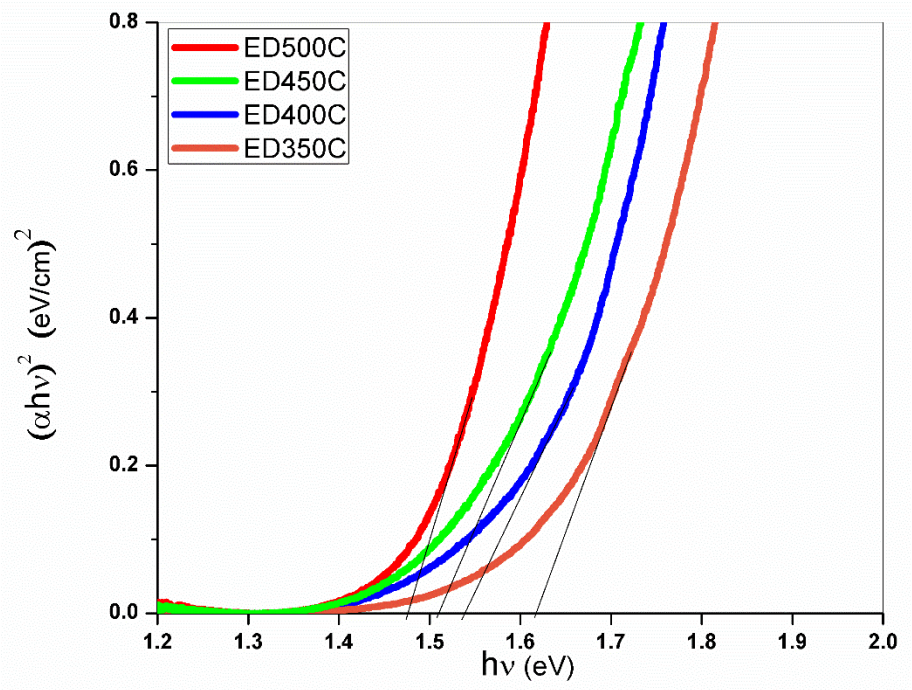

Figure 8: CZTS thin film band gap energy

Table 4: CZTS thin films optical band gaps

Samples	Annealing Temperature (℃)	Optical band gap (eV)
ED400C	400	1.61
ED450C	450	1.54
ED500C	500	1.51
ED550C	550	1.48

4. Conclusion

In this work CZTS thin film is fabricated using electrochemical deposition. The major concern for the limitation to achieve high efficiency CZTS thin film is to control the composition of metal alloys as these alloys has different oxidization and reduction potential. To control the composition of the alloys and to get good stoichiometry of the film trisodium citrate $C_6H_5Na_3O_7$ complexing agent was added into the solution with $0.2\ M$ concentration. From the results presented above it was found that 0.2M molar concentration works well for the fabrication of CZTS thin film with good structural, morphological and optical properties at different annealing temperatures ($400℃ - 550℃$). The thin film with good morphological, structural and optical ($1.51eV$) properties was achieved at temperature $500℃$.

ACKNOWLEDGMENTS

This work was supported by Ministerio de Economía y Competitividad (ENE2016-77798-C4-2-R) and Generalitat Valenciana (Prometeus 2014/044).

References:

[1] M. Powalla, S. Paetel, D. Hariskos, R. Wuerz, F. Kessler, P. Lechner, W. Wischmann, T.M. Friedlmeier, Advances in Cost-Efficient Thin-Film Photovoltaics Based on Cu(In,Ga)Se 2, Engineering. 3 (2017) 445–451. doi:10.1016/J.ENG.2017.04.015.

[2] Y.H. Khattak, F. Baig, S. Ullah, B. Marí, S. Beg, H. Ullah, Enhancement of the conversion efficiency of thin film kesterite solar cell, J. Renew. Sustain. Energy. 10 (2018) 03350101–033514. doi:10.1063/1.5023478.

[3] M.H. Rashid, J. Rabeya, M.H. Doha, O. Islam, P. Reith, G. Hopman, H. Hilgenkamp, Characterization of single step electrodeposited Cu2ZnSnS4 thin films, J. Opt. 47 (2018) 256–262. doi:10.1007/s12596-018-0463-0.

[4] F. Jiang, S. Li, C. Ozaki, T. Harada, S. Ikeda, Co-Electrodeposited Cu 2 ZnSnS 4 Thin Film Solar Cell and Cu 2 ZnSnS 4 Solar Cell - BiVO 4 Tandem Device for Unbiased Solar Water Splitting, Sol. RRL. 2 (2018) 1700205. doi:10.1002/solr.201700205.

[5] J.-M. Delgado-Sanchez, J.M. López-González, A. Orpella, E. Sánchez-Cortezon, M.D. Alba, C. López-López, R. Alcubilla, Front contact optimization of industrial scale CIGS solar cells for low solar concentration using 2D physical modeling, Renew. Energy. 101 (2017) 90–95. doi:10.1016/j.renene.2016.08.046.

[6] Y.H. Khattak, F. Baig, S. Ullah, B. Marí, S. Beg, H. Ullah, Numerical modeling baseline for high efficiency (Cu 2 FeSnS 4) CFTS based thin film kesterite solar cell, Optik (Stuttg). 164 (2018) 547–555. doi:10.1016/j.ijleo.2018.03.055.

[7] I.L. Repins, M.J. Romero, J. V. Li, S.-H. Wei, D. Kuciauskas, C.-S. Jiang, C. Beall, C. DeHart, J. Mann, W.-C. Hsu, G. Teeter, A. Goodrich, R. Noufi, Kesterite Successes, Ongoing Work, and Challenges: A Perspective From Vacuum Deposition, IEEE J. Photovoltaics. 3 (2013) 439–445. doi:10.1109/JPHOTOV.2012.2215842.

[8] H. Wang, Y. Liu, M. Li, H. Huang, H.M. Xu, R.J. Hong, H. Shen, Multifunctional TiO2nanowires-modified nanoparticles bilayer film for 3D dye-sensitized solar cells, Optoelectron. Adv. Mater. Rapid Commun. 4 (2010) 1166–1169. doi:10.1039/b000000x.

[9] H. Zhou, W.-C.C. Hsu, H.-S.S. Duan, B. Bob, W. Yang, T.-B. Bin Song, C.-J.J. Hsu, Y. Yang, CZTS nanocrystals: a promising approach for next generation thin film photovoltaics, Energy Environ. Sci. 6 (2013) 2822. doi:10.1039/c3ee41627e.

[10] Y.H. Khattak, F. Baig, B. Marí, S. Beg, S.R. Gillani, T. Ahmed, Effect of CdTe Back Surface Field on the Efficiency Enhancement of a CGS Based Thin Film Solar Cell, J. Electron. Mater. 47 (2018) 5183–5190. doi:10.1007/s11664-018-6405-4.

[11] S.K. Swami, A. Kumar, V. Dutta, Deposition of Kesterite Cu2ZnSnS4 (CZTS) Thin Films by Spin Coating Technique for Solar Cell Application, Energy Procedia. 33 (2013) 198–202. doi:10.1016/j.egypro.2013.05.058.

[12] K. Tanaka, N. Moritake, H. Uchiki, Preparation of Cu2ZnSnS4 thin films by sulfurizing sol–gel deposited precursors, Sol. Energy Mater. Sol. Cells. 91 (2007) 1199–1201. doi:10.1016/j.solmat.2007.04.012.

[13] H. Saïdi, M.F. Boujmil, B. Durand, J.-L. Lazzari, M. Bouaïcha, Elaboration and characterization of CuInSe 2 thin films using one-step electrodeposition method on silicon substrate for photovoltaic application, Mater. Res. Express. 5 (2018) 016414. doi:10.1088/2053-1591/aaa604.

[14] N. Kamoun, H. Bouzouita, B. Rezig, Fabrication and characterization of Cu2ZnSnS4 thin films deposited by spray pyrolysis technique, Thin Solid Films. 515 (2007) 5949–5952. doi:10.1016/j.tsf.2006.12.144.

[15] M.I. Amal, S.H. Lee, K.H. Kim, Properties of Cu2ZnSn(SxSe1−x)4 thin films prepared by one-step sulfo-selenization of alloyed metal precursors, Curr. Appl. Phys. 14 (2014) 916–921. doi:10.1016/j.cap.2014.04.005.

[16] T.P. Dhakal, C. Peng, R. Reid Tobias, R. Dasharathy, C.R. Westgate, Characterization of a CZTS thin film solar cell grown by sputtering method, Sol. Energy. 100 (2014) 23–30. doi:10.1016/j.solener.2013.11.035.

[17] Y. Lu, S. Wang, X. Ma, X. Xu, S. Yang, Y. Li, Z. Tang, The characteristic of Cu2ZnSnS4 thin film solar cells prepared by sputtering CuSn and CuZn alloy targets, Curr. Appl. Phys. 18 (2018) 1571–1576. doi:10.1016/j.cap.2018.10.005.

[18] T.R. Rana, N.M. Shinde, J. Kim, Novel chemical route for chemical bath deposition of Cu2ZnSnS4 (CZTS) thin films with stacked precursor thin films, Mater. Lett. 162 (2016) 40–43. doi:10.1016/j.matlet.2015.09.100.

[19] J. Henry, K. Mohanraj, G. Sivakumar, Electrical and optical properties of CZTS thin films prepared by SILAR method, J. Asian Ceram. Soc. 4 (2016) 81–84. doi:10.1016/j.jascer.2015.12.003.

[20] K. Moriya, J. Watabe, K. Tanaka, H. Uchiki, Characterization of Cu2ZnSnS4 thin films prepared by photo-chemical deposition, Phys. Status Solidi. 3 (2006) 2848–2852. doi:10.1002/pssc.200669588.

[21] W. Wang, M.T. Winkler, O. Gunawan, T. Gokmen, T.K. Todorov, Y. Zhu, D.B. Mitzi, Device characteristics of CZTSSe thin-film solar cells with 12.6% efficiency, Adv. Energy Mater. 4 (2014) 1–5. doi:10.1002/aenm.201301465.

[22] Y.S. Lee, T. Gershon, O. Gunawan, T.K. Todorov, T. Gokmen, Y. Virgus, S. Guha, Cu2ZnSnSe4 thin-film solar cells by thermal co-evaporation with 11.6% efficiency and improved minority carrier diffusion length, Adv. Energy Mater. 5 (2015). doi:10.1002/aenm.201401372.

[23] D.J. Coyle, H.A. Blaydes, R.S. Northey, J.E. Pickett, K.R. Nagarkar, R. Zhao, J.O. Gardner,

Life prediction for CIGS solar modules part 2, Prog. Photovoltaics. (2013) 156–172. doi:10.1002/pip.

[24] C. Yan, J. Huang, K. Sun, S. Johnston, Y. Zhang, H. Sun, A. Pu, M. He, F. Liu, K. Eder, L. Yang, J.M. Cairney, N.J. Ekins-Daukes, Z. Hameiri, J.A. Stride, S. Chen, M.A. Green, X. Hao, Cu 2 ZnSnS 4 solar cells with over 10% power conversion efficiency enabled by heterojunction heat treatment, Nat. Energy. 3 (2018) 764–772. doi:10.1038/s41560-018-0206-0.

[25] F. Jiang, S. Ikeda, T. Harada, M. Matsumura, Pure Sulfide Cu2ZnSnS4 thin film solar cells fabricated by preheating an electrodeposited metallic stack, Adv. Energy Mater. 4 (2014) 2–5. doi:10.1002/aenm.201301381.

[26] S. Ahmed, K.B. Reuter, O. Gunawan, L. Guo, L.T. Romankiw, H. Deligianni, A High Efficiency Electrodeposited Cu2ZnSnS4 Solar Cell, Adv. Energy Mater. 2 (2012) 253–259. doi:10.1002/aenm.201100526.

[27] Y. Lin, S. Ikeda, W. Septina, Y. Kawasaki, T. Harada, M. Matsumura, Mechanistic aspects of preheating effects of electrodeposited metallic precursors on structural and photovoltaic properties of Cu2ZnSnS4 thin films, Sol. Energy Mater. Sol. Cells. 120 (2014) 218–225. doi:10.1016/j.solmat.2013.09.006.

[28] J. Tao, J. Liu, J. He, K. Zhang, J. Jiang, L. Sun, P. Yang, J. Chu, Synthesis and characterization of Cu 2 ZnSnS 4 thin films by the sulfurization of co-electrodeposited Cu–Zn–Sn–S precursor layers for solar cell applications, RSC Adv. 4 (2014) 23977–23984. doi:10.1039/C4RA02327G.

[29] J. Tao, J. He, K. Zhang, J. Liu, Y. Dong, L. Sun, P. Yang, J. Chu, Effect of deposition potential on the properties of Cu 2 ZnSnS 4 films for solar cell applications, 135 (2014) 8–10. doi:10.1016/j.matlet.2014.07.144.

[30] H. Kirou, L. Atourki, A. Almaggoussi, K. Abouabassi, A. Soltani, A. Almaggoussi, A. Elfanaoui, K. Bouabid, M. Nya, A. Ihlal, Effects of Na2SO4 on the optical and structural properties of Cu2ZnSnS4 thin films synthesized using co-electrodeposition technique, Opt. Mater. (Amst). 75 (2018) 471–482. doi:10.1016/j.optmat.2017.11.004.

[31] R. Sani, R. Manivannan, S.N. Victoria, One step electrochemical deposition of CZTS for solar cell applications, 9 (2018) 165–170. doi:10.5229/Jesct.2018.9.4.308.

[32] D.B. Mitzi, O. Gunawan, T.K. Todorov, K. Wang, S. Guha, Solar Energy Materials & Solar Cells The path towards a high-performance solution-processed kesterite solar cell $, Sol. Energy Mater. Sol. Cells. 95 (2011) 1421–1436. doi:10.1016/j.solmat.2010.11.028.

[33] J. Tao, J. Liu, J. He, K. Zhang, J. Jiang, L. Sun, RSC Advances Cu – Zn – Sn – S precursor layers for solar cell, (2014) 23977–23984. doi:10.1039/c4ra02327g.

[34] A. Tang, J. Liu, J. Ji, M. Dou, Z. Li, F. Wang, Applied Surface Science One-step electrodeposition for targeted off-stoichiometry Cu 2 ZnSnS 4 thin films, Appl. Surf. Sci. 383 (2016) 253–260. doi:10.1016/j.apsusc.2016.04.189.

[35] S.G. Lee, J. Kim, H.S. Woo, Y. Jo, A.I. Inamdar, S.M. Pawar, H.S. Kim, W. Jung, H.S. Im, Structural, morphological, compositional, and optical properties of single step electrodeposited Cu2ZnSnS4 (CZTS) thin films for solar cell application, Curr. Appl. Phys. 14 (2014) 254–258. doi:10.1016/j.cap.2013.11.028.

[36] J. Tao, J. Liu, L. Chen, H. Cao, X. Meng, Y. Zhang, C. Zhang, L. Sun, P. Yang, J. Chu, 7.1% efficient co-electroplated Cu 2 ZnSnS 4 thin film solar cells with sputtered CdS buffer layers, Green Chem. 18 (2016) 550–557. doi:10.1039/C5GC02057C.

[37] B. Rezaei, N. Irannejad, A.A. Ensafi, 3D TiO2 self-acting system based on dye-sensitized solar cell and g-C3N4/TiO2-MIP to enhanced photodegradation performance, Renew. Energy. 123 (2018) 281–293. doi:10.1016/j.renene.2018.02.042.

[38] T. Slimani Tlemcani, F.C. El Moursli, M. Taibi, F. Hajji, E.B. Benamar, S. Colis, G. Schmerber, D. Muller, A. Slaoui, A. Dinia, M. Abd-Lefdil, One step electrodeposited CZTS thin films: Preparation and characterization, in: 2014 Int. Renew. Sustain. Energy Conf., IEEE, 2014: pp. 89–93. doi:10.1109/IRSEC.2014.7059867.

[39] S.R. Kodigala, The Role of Characterization Techniques in the Thin Film Analysis, in: Thin Film Sol. Cells From Earth Abund. Mater., Elsevier, 2014: pp. 67–140. doi:10.1016/B978-0-12-394429-0.00004-4.

[40] C.W. Hong, S.W. Shin, M.P. Suryawanshi, M.G. Gang, J. Heo, J.H. Kim, Chemically Deposited CdS Buffer/Kesterite Cu 2 ZnSnS 4 Solar Cells: Relationship between CdS Thickness and Device Performance, ACS Appl. Mater. Interfaces. 9 (2017) 36733–36744. doi:10.1021/acsami.7b09266.

[41] F.W. Gayle, F.S. Biancaniello, STACKING FAULTS AND CRYSTALLITE SIZE, 6 (1995) 429–432.

[42] R. Touati, M. Ben Rabeh, M. Kanzari, Structural and Optical Properties of the New Absorber Cu2ZnSnS4 Thin Films Grown by Vacuum Evaporation Method, Energy Procedia. 44 (2014) 44–51. doi:10.1016/j.egypro.2013.12.008.

[43] H. Shang, Y. Zhang, Y. Li, Y. Qi, S. Guo, D. Zhao, Effects of adding over-stoichiometrical Ti and substituting Fe with Mn partly on structure and hydrogen storage performances of TiFe alloy, Renew. Energy. 135 (2019) 1481–1498. doi:10.1016/j.renene.2018.09.072.

[44] N. Soundaram, R. Chandramohan, S. Valanarasu, R. Thomas, A. Kathalingam, Studies on SILAR deposited Cu2O and ZnO films for solar cell applications, J. Mater. Sci. Mater. Electron. 26 (2015) 5030–5036. doi:10.1007/s10854-015-3020-5.

[45] S. Rondiya, A. Rokade, A. Jadhavar, S. Nair, M. Chaudhari, R. Kulkarni, A. Mayabadi, A. Funde, H. Pathan, S. Jadkar, Effect of calcination temperature on the properties of CZTS absorber layer prepared by RF sputtering for solar cell applications, Mater. Renew. Sustain. Energy. 6 (2017) 8. doi:10.1007/s40243-017-0092-6.

[46] Z. Su, C. Yan, K. Sun, Z. Han, F. Liu, J. Liu, Y. Lai, J. Li, Y. Liu, Preparation of Cu2ZnSnS4 thin films by sulfurizing stacked precursor thin films via successive ionic layer adsorption and reaction method, Appl. Surf. Sci. 258 (2012) 7678–7682. doi:10.1016/j.apsusc.2012.04.120.

[47] P.A. Fernandes, P.M.P. Salomé, A.F. da Cunha, Growth and Raman scattering characterization of Cu2ZnSnS4 thin films, Thin Solid Films. 517 (2009) 2519–2523. doi:10.1016/j.tsf.2008.11.031.

[48] S.W. Shin, I.Y. Kim, K.V. Gurav, C.H. Jeong, J.H. Yun, P.S. Patil, J.Y. Lee, J.H. Kim, Band gap tunable and improved microstructure characteristics of Cu2ZnSn(S1−x,Sex)4 thin films by annealing under atmosphere containing S and Se, Curr. Appl. Phys. 13 (2013) 1837–1843. doi:10.1016/j.cap.2013.06.022.

[49] A. Khare, A.W. Wills, L.M. Ammerman, D.J. Norris, E.S. Aydil, Size control and quantum confinement in Cu2ZnSnS4nanocrystals, Chem. Commun. 47 (2011) 11721–11723. doi:10.1039/c1cc14687d.